Monoclonal Antibody Blockade of the Human Eag1 Potassium Channel Function Exerts Antitumor Activity

David Gómez-Varela,[1] Esther Zwick-Wallasch,[3] Hendrik Knötgen,[2] Araceli Sánchez,[1] Thore Hettmann,[3] Dmitri Ossipov,[2] Rüdiger Weseloh,[1] Constanza Contreras-Jurado,[1] Mike Rothe,[3] Walter Stühmer,[1] and Luis A. Pardo[1]

[1]Max-Planck Institute of Experimental Medicine, and [2]iOnGen AG, Göttingen, Germany; and [3]U3 Pharma AG, Martinsried, Germany

Abstract

The potassium channel ether à go-go has been directly linked to cellular proliferation and transformation, although its physiologic role(s) are as of yet unknown. The specific blockade of human Eag1 (hEag1) may not only allow the dissection of the role of the channel in distinct physiologic processes, but because of the implication of hEag1 in tumor biology, it may also offer an opportunity for the treatment of cancer. However, members of the potassium channel superfamily are structurally very similar to one another, and it has been notoriously difficult to obtain specific blockers for any given channel. Here, we describe and validate the first rational design of a monoclonal antibody that selectively inhibits a potassium current in intact cells. Specifically blocking hEag1 function using this antibody inhibits tumor cell growth both *in vitro* and *in vivo*. Our data provide a proof of concept that enables the generation of functional antagonistic monoclonal antibodies against ion channels with therapeutic potential. The particular antibody described here, as well as the technique developed to make additional functional antibodies to Eag1, makes it possible to evaluate the potential of the channel as a target for cancer therapy. [Cancer Res 2007;67(15):7343–9]

Introduction

There is compelling evidence that potassium channels play an important role in fundamental cellular processes such as excitability, muscle contraction, cell cycle progression, and cellular proliferation (1–3). Human Eag1 (hEag1) Kv10.1 in the International Union of Pharmacology nomenclature; ref. (4), encoded by the *KCNH1* gene) is a voltage-gated potassium channel modulated throughout the cell cycle (5, 6) and has been suggested to be involved in tumorigenesis. It has been shown that ectopic expression of hEag1 favors tumor progression when transfected cells are injected in immunodepressed mice (7). Conversely, antisense or RNAi-mediated inhibition of hEag1 expression in tumor cell lines causes extensive reduction of cell proliferation (7, 8). Similarly, inhibition of hEag1-mediated currents by nonselective channel blockers like imipramine and astemizole has been suggested to decrease cell proliferation in melanoma and breast cancer cells (9, 10). In addition, the expression of human hEag1 has been detected in many tumor cell lines *in vitro* and in tumor tissues from cancer patients across all major tumor types (11–13), whereas the normal expression of hEag1 in healthy human tissues is preferentially confined to the central nervous system (7, 12, 14). These observations prompt the possibility that hEag1 channels participate in the progression of the malignant disease and thus represent a valid target for therapeutic intervention.

A vast number of unspecific and nonselective drugs that modulate the activity of various types of potassium channels are available. However, the homogeneous structural features of the entire voltage-gated potassium channel superfamily make it difficult to identify selective blockers (15). Specifically, the closest homologue of hEag1 is human Eag2 (16), which displays 73% amino acid sequence identity with hEag1, the highest divergence being concentrated within the cytoplasmic COOH termini (16, 17). Moreover, an important member of the EAG channel family is the human ether à go-go–related channel (HERG; ref. 18), the inhibition of which triggers well-characterized and dangerous cardiac consequences (19). Consequently, selectivity is a crucial feature for any potential anti-hEag1 therapy, as all currently known hEag1 blockers inhibit HERG to various degrees (20, 21).

Monoclonal antibodies represent a strategy to generate highly selective inhibitors against cell surface molecules, enabling a specific antigen to be distinguished from its closest homologues. Some polyclonal sera have been produced that effectively inhibit potassium currents in intact cells (15, 22). Unfortunately, polyclonal antibodies have the disadvantage that even after a serum has successfully been generated, there is no guarantee that another effective blocker can be produced using the same strategy (23, 24). The exquisite selectivity of monoclonal antibodies, however, could be exploited to generate molecules with the required target specificity, and advantageously, rational design processes can be incorporated into their development. Additionally, monoclonal antibodies can generally be produced in a recombinant system and modified to render them usable for therapeutic approaches. Therefore, we have designed a rational approach to produce the first monoclonal antibody that specifically inhibits a potassium channel in intact cells and thereby exerts antitumor effects.

Materials and Methods

Electrophysiology. For electrophysiologic experiments, monoclonal HEK293 cells expressing hEag1 (21) were grown for 24 to 72 h on poly L-lysine–coated glass coverslips. All electrophysiologic experiments were done at room temperature. Macroscopic currents were recorded in the whole-cell configuration of the patch-clamp technique using an EPC-9 amplifier and Pulse software (HEKA). Patch pipettes with a tip resistance of 1.5 to 2 MΩ were made from Corning no. 0010 capillary glass (WPI). The internal solution contained 100 mmol/L of KCl, 45 mmol/L of N-methyl-D-glucamine, 10 mmol/L of 1,2-bis(2-aminophenoxy)ethane-N,N,N,N-tetra-acetic acid tetrapotassium salt (BAPTA·K_4), and 10 mmol/L of HEPES/HCl (pH 7.35). The control external recording solution contained 160 mmol/L of

Note: D. Gómez-Varela and E. Zwick-Wallasch contributed equally to this work.

Requests for reprints: Luis Pardo, Max-Planck Institute of Experimental Medicine, Hermann-Rein-Str. 3, 37075 Göttingen, Germany. E-mail: pardo@em.mpg.de.

doi:10.1158/0008-5472.CAN-07-0107

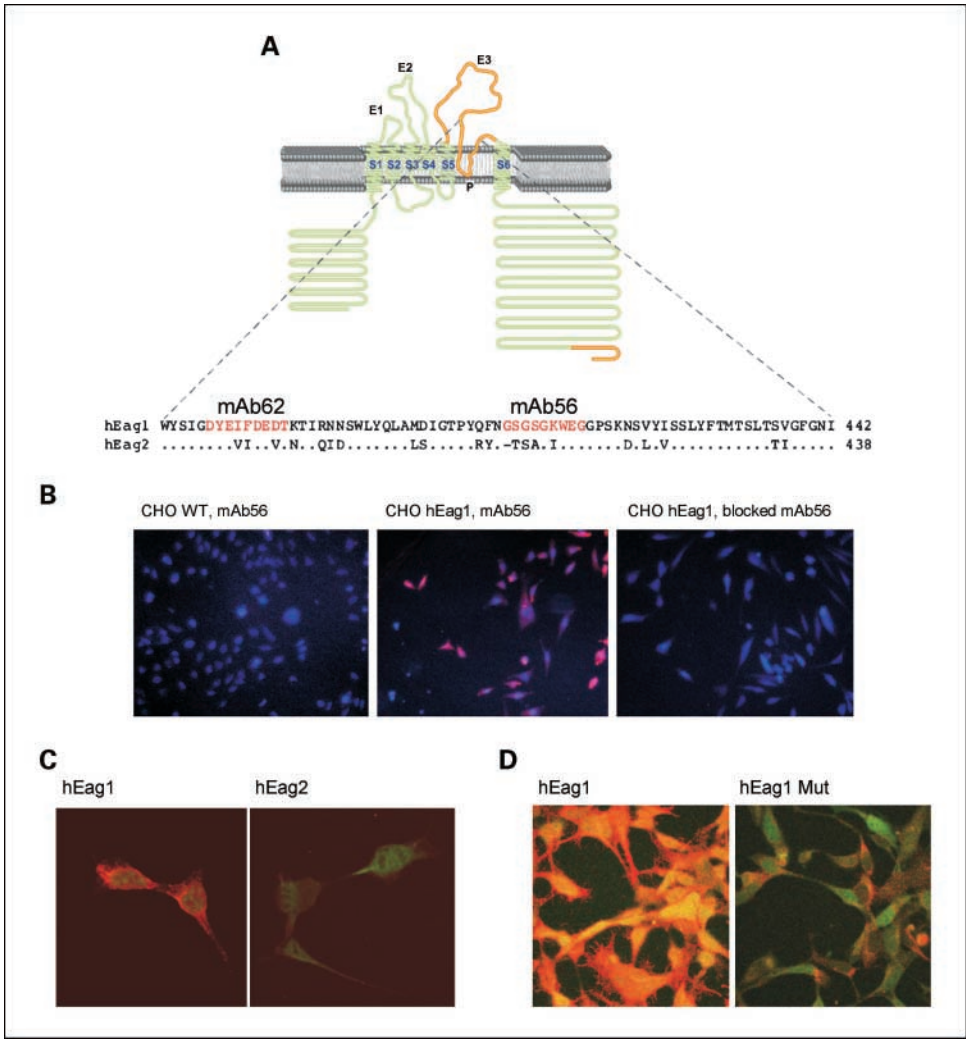

Figure 1. *A,* putative topology of the monomer of the Eag K^+ channel family. The regions used to generate mAb56 are highlighted. An alignment of the E3 regions of hEag1 and hEag2 is also shown with the epitopes of mAb56 and mAb62 (*red*). *B,* specific detection of hEag1 with mAb56. Confocal images of CHO cells transfected with hEag1. The staining only appears in the transfected cell line and not in control cells or after incubation of mAb56 with its specific epitope (4′,6-diamidino-2-phenylindole counterstain; magnification, ×20). *C,* mAb56 does not recognize hEag2. Cells transfected with hEag2 show only background staining with mAb56 (AlexaFluor 546 secondary antibody; *green,* green fluorescent protein from the pTracerCMV vector). *D,* mutation of the epitope for mAb56 abolishes the detection of channels in transfected HEK293 cells. Cells were transfected with wild-type hEag1 or a mutant hEag1 channel in which the mAb56 epitope had been modified to the hEag2 sequence. Cells were thereafter stained using mAb56 and a secondary antibody coupled to AlexaFluor 546.

NaCl, 2.5 mmol/L of KCl, 2 mmol/L of $CaCl_2$, 1 mmol/L of $MgCl_2$, 8 mmol/L of glucose, and 10 mmol/L of HEPES/NaOH (pH 7.4). Series resistance was determined using the automated capacity compensation of the amplifier and compensated by 60% to 80%. Data were analyzed using PulseFit and IgorPro (WaveMetrics). Data shown in text and legends represent mean ± SE for the indicated number of experiments. Statistical analysis was done using Student's *t* test for a two-tailed distribution.

Immunofluorescence. Immunofluorescence was done on transfected CHO-K1 and HEK293 cells grown on glass coverslips. Cells were washed thrice with TBS (150 mmol/L NaCl, 20 mmol/L Tris-HCl; pH 7.5), fixed with 4% *p*-formaldehyde (4°C for 4 min), and permeabilized with 1% Triton X-100 in TBS for 10 min. Nonspecific binding was blocked with 10% bovine serum albumin in TBS for 30 min. Primary antibody (1 μg/mL) incubation was done at room temperature for 2 h. AlexaFluor 546–labeled anti-mouse IgG antibody (Molecular Probes) was used as a secondary antibody. The coverslips were mounted using ProLong (Molecular Probes) and observed in a Zeiss LSM 510 laser-scanning confocal microscope.

Site-directed mutagenesis. Mutations on the epitope sequence of hEag1 were introduced with the QuickChange XL site-directed mutagenesis kit (Stratagene) using primers with the sequences: 5′-CAGTTTAATGGG-TCTGCCGGGATTTGGGAAGGTGGTCC and 5′-GGACCACCTTCCCAAATC-CCGGCAGACCCATTAAACTG. Afterwards, the complete coding sequence was confirmed to discard additional mutations.

Colony formation assay. Cells were preincubated with the corresponding antibody or vehicle and resuspended in 50 μL of 0.25% Noble agar (Difco) containing OptiMEM and 0.5% FCS. The suspension was plated on an agarose underlayer (OptiMEM with 20% FCS and 0.5% agarose, 50 μL) in quadruplicate wells of a 96-well plate. A 50 μL feeding layer (OptiMEM with 0.5% FCS) was plated on top of each well. Colonies were allowed to grow in the presence of antibody for 7 to 8 days and then stained with 50 μL of 3-(4,5-dimethylthiazol-2-yl)-2,5-diphenyltetrazolium bromide (1 mg/mL in PBS) for 3 to 6 h. Viable colonies develop blue color through metabolization of 3-(4,5-dimethylthiazol-2-yl)-2,5-diphenyltetrazolium bromide and are thereby readily detectable. Wells were scanned in a LemnaTec Scanalyzer 3D System and the number of colonies was counted using the corresponding software.

Animal experiments. For *in vivo* tumor growth inhibition studies, we used xenograft implants in immunodeficient mice. In the MDA-MB-435S human breast cancer model, female CB17 Fox Chase severe combined immunodeficiency (SCID) mice (~20 g body weight) were implanted with 10^7 cells in 200 μL of PBS. After measurable tumors developed, the animals were randomized into groups of 10 individuals with comparable average tumor size and body weight. After randomization, a loading mAb56 dose of 50 mg/kg, followed by weekly doses of 25 mg/kg was administered i.p. A negative control group received the same volume of PBS. As a positive control, cyclophosphamide (6.25 mg/kg) was administered orally. Tumor size was determined twice a week, always by the same operator, and tumor volume was estimated by multiplying the larger diameter by the square of the shorter diameter and the correction factor 0.52.

For the human pancreas carcinoma model PAXF1657, two groups of tumor-bearing nude mice (10 mice/group) received mAb56 or mAb33 i.p. at a loading dose of 50 mg/kg/d and follow-up dosing of 25 mg/kg/d on days 4,

7, and 11. A third group served as a positive control and was treated with i.v. gemcitabine at 200 mg/kg/d on days 0 and 7. The fourth group received vehicle (PBS) i.p. on days 4, 7, and 11. Tumor sizes were measured twice a week. In Fig. 5, sizes are given as the median relative to the volume at start of treatment. Error bars in Figs. 2, 3 and 4 represent SE.

Results and Discussion

Antibody generation. For the optimal immunogen design, we compared the sequences of hEag1, hEag2, and HERG in order to avoid cross-reactivity. We then concentrated on two regions of the channel, the linker between the fifth and sixth putative transmembrane segments (segment E3; Fig. 1*A*; ref. 15), and the COOH-terminal end. The E3 segment was chosen under the assumption that it should be the area closest to the ion permeation route from the extracellular side. This region has been successfully used to generate polyclonal antibodies against several ion channels (15, 22). The COOH-terminal end of the hEag1, putatively intracellular, should not play a direct role in the generation of a functional antibody, but it contains a segment that induces tetramerization (the tetramerizing coiled-coil; refs. 25, 26). This would mimic the structure of the natural channel because hEag1 is, like most potassium channels, a tetramer. The three-dimensional structure of the antigen can be very important in the immune process (27).

We thus generated a fusion protein containing two domains (Fig. 1*A*), residues 374 to 452, including the E3 segment, and residues 872 to 932, including the tetramerizing coiled-coil.

After immunization with this fusion protein and the generation of hybridomas using standard procedures (12), we defined a multilevel selection protocol to screen for functional antibodies. First, the supernatants showing highest affinity for the recombinant antigen in ELISA assays were tested by surface plasmon resonance (SPR; ref. 28) to determine which part of the immunogen contained the epitope. Those recognizing the E3 region were subsequently tested for their ability to distinguish between

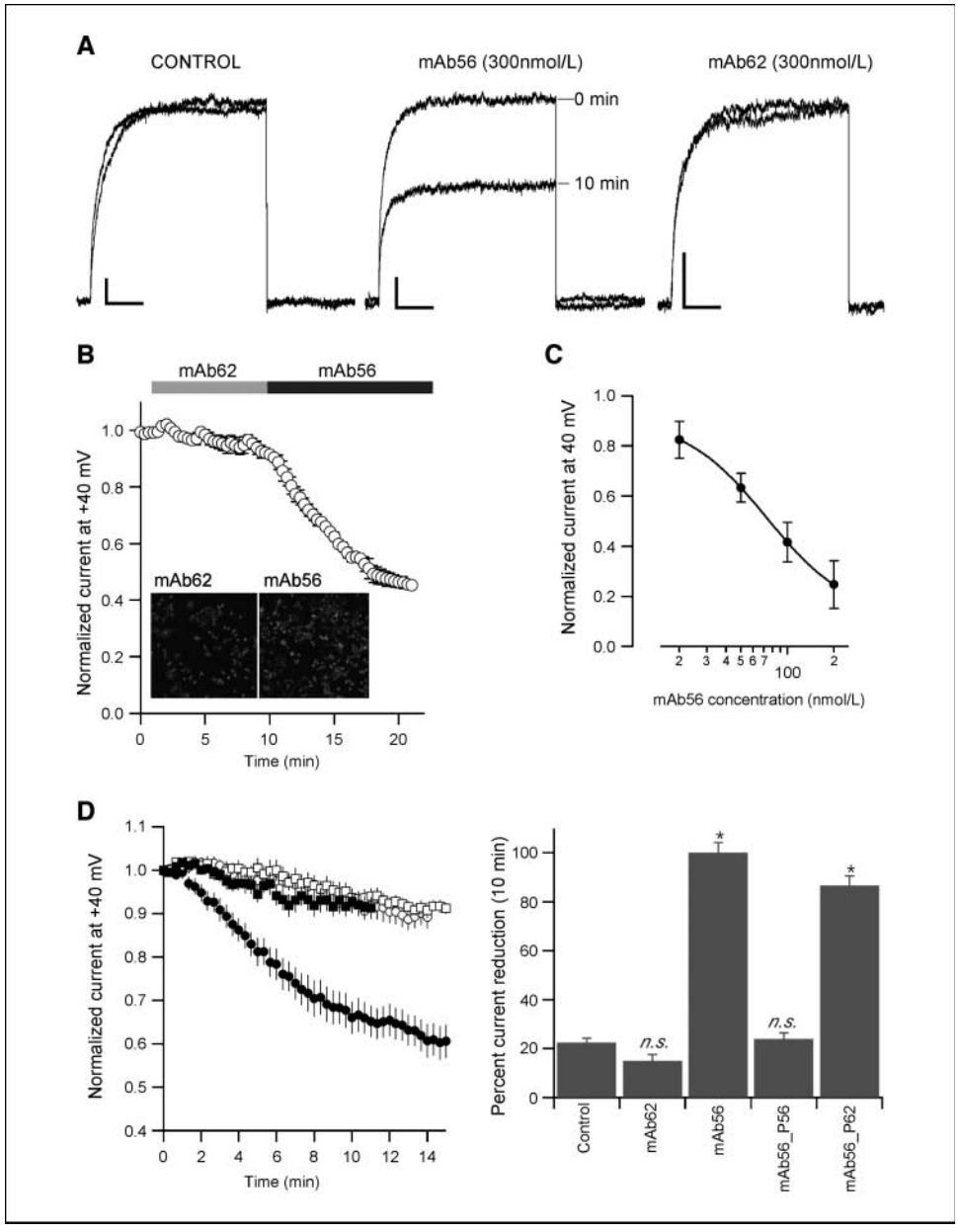

Figure 2. *A,* mAb56 reduces hEag1 currents. Perfusion of 300 nmol/L of mAb56 for 10 min reduces the hEag1 current in transfected HEK293 cells. Currents were elicited by a 1-s depolarization to +40 mV from a holding potential of −80 mV. The effect was absent when cells were perfused with vehicle (*control*) or with 300 nmol/L of mAb62 (*mAb62*). *Bars,* 500 pA, 200 ms. *B,* consecutive application of 300 nmol/L of mAb62 and mAb56. mAb56 reduces the current amplitude (55 ± 0.5%), whereas mAb62 fails to induce any effect (8 ± 1.6%; $n = 3$). Data normalized to the current at the end of the +40 mV step before mAb62 application. *Inset,* both antibodies recognize the channel in HEK293 cells. *C,* dose-response relationship of the inhibitory effect of mAb56 on hEag1 currents expressed in HEK293 cells ($n = 3$). Current amplitude was measured at the steady state under continuous perfusion of the antibody-containing solution. *D,* time course of the reduction of current amplitude in control cells (○, $n = 13$), cells perfused with mAb56 (●, $n = 14$), with peptide-blocked mAb56 (■, $n = 6$), or with mAb62 (□, $n = 8$). Data were obtained as in (*B*) using 300 nmol/L of each antibody. Quantification of the effects of mAb56 and mAb62, and mAb56 treated with peptides corresponding to either the cognate epitope or that of mAb62 (*right*). Data are presented normalized to the block achieved with mAb56 (34 ± 4.2%; $n = 14$) after 10 min; the recorded blockade levels were 7.5 ± 1.9% ($n = 13$) for the controls, 5 ± 2.7% ($n = 7$) for mAb62, 8 ± 2.5% ($n = 6$) for mAb56 preincubated with its epitope (*P56*), and 29 ± 4% ($n = 7$) for mAb56 preincubated with the mAb62 epitope (*P62*). *, $P < 0.01$ in a two-tailed *t* test against controls.

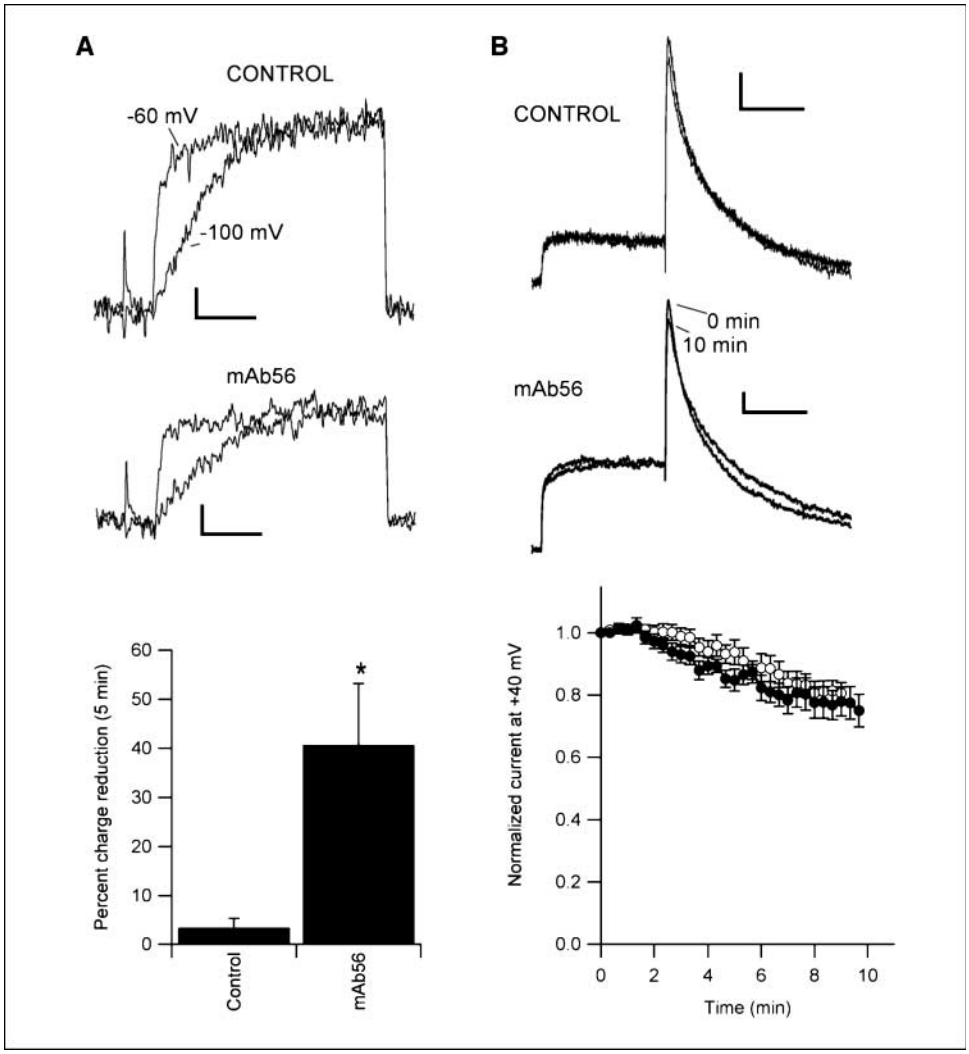

Figure 3. *A,* endogenous hEag1 currents were reduced by mAb56 in SH-SY5Y cells. Currents were detected by the Cole-Moore shift, after 5 min of treatment with vehicle (*control*) or 300 nmol/L of mAb56 (*mAb56*) using a 1-s depolarization to +40 mV from holding potentials of −60 or −100 mV. The difference in charge displacement elicited at +40 mV from the two different holding potentials represents the hEag1 current component (7). mAb56 (300 nmol/L) treatment produced a 44.7 ± 12% (n = 4) reduction in this component (versus 3.4 ± 1.9% in controls; n = 4). *Bars,* 20 pA. 100 ms. *B,* mAb56 does not block HERG channels. Representative HERG currents elicited by 1-s depolarization to + 40 mV from a holding potential of −80 mV and return to −75 mV (*bars,* 200 pA, 500 ms) mAb56 (300 nmol/L) did not reduce the current after 10 min of treatment. Current, measured at the peak amplitude of the −75 mV segment, was normalized to the current level of the first pulse. Normalized values, after 10 min, were reduced by 20 ± 3% (n = 10) and 22 ± 5% (n = 6) for control and mAb56-treated cells, respectively.

epitopes from hEag1 and hEag2 in ELISA and SPR. The hybridomas that qualified were then tested for functional inhibition of hEag1 currents in *Xenopus* oocytes (29). Only one of the supernatants (mAb56) reduced hEag1 currents significantly. The hybridoma was then re-cloned and the antibody produced was purified by double affinity chromatography (protein A and specific antigen). We then proceeded to a more detailed characterization of the properties of this particular antibody.

Antibody characterization. Epitope mapping using an array of overlapping peptides spanning the complete region of interest revealed that the region recognized by mAb56 was linear and corresponds to the sequence: GSGSGKWEG. Alignments to hEag2 (Fig. 1*A*) show that only four residues in the epitope are conserved between the two channels. BLAST searches using the epitope sequence did not reveal significant similarity with any other protein. When the performance of mAb56 was tested in immunofluorescence, we found clear positive signals in CHO, HEK293, and NIH3T3 cells expressing hEag1, which could be completely blocked by preincubation of the antibody with an excess of the peptide corresponding to the mAb56 epitope (Fig. 1*B*).

No signal was detected in immunofluorescence experiments on HEK293 cells overexpressing either hEag2 (Fig. 1*C*) or a mutant hEag1 channel derivative in which the mAb56 epitope had been mutated to the hEag2 sequence (Fig. 1*D*). Additionally, we have found no evidence for nonspecific bands using mAb56 in Western blots, although the antibody's sensitivity is relatively low in this assay. The lack of cross-reactivity in SPR, together with the low sequence similarity of the epitope and the immunofluorescence results, suggest a specific interaction with hEag1.

Effects of mAb56 on hEag1 electrophysiology. We subsequently tested the ability of mAb56 to inhibit hEag1 current expressed in HEK293 cells using whole-cell patch clamp (30). Superfusion of mAb56 (45 μg/mL; ~300 nmol/L) induced an inhibition of ~40% of the current amplitude in 10 min (Fig. 2*A*), a period of time that did not induce remarkable rundown in the absence of the antibody. Both in HEK293 cells and in *Xenopus* oocytes, activation of the channel was required to observe antibody-mediated inhibition. When the cells were preincubated for 10 min after the addition of the antibody, and before applying a depolarizing pulse, the current amplitude was unaffected, indicating voltage-dependence of the blocking effect of the antibody (data not shown).

The ability to inhibit the ionic current is specific to mAb56. Another monoclonal antibody (mAb62; refs. 12, 31) raised against

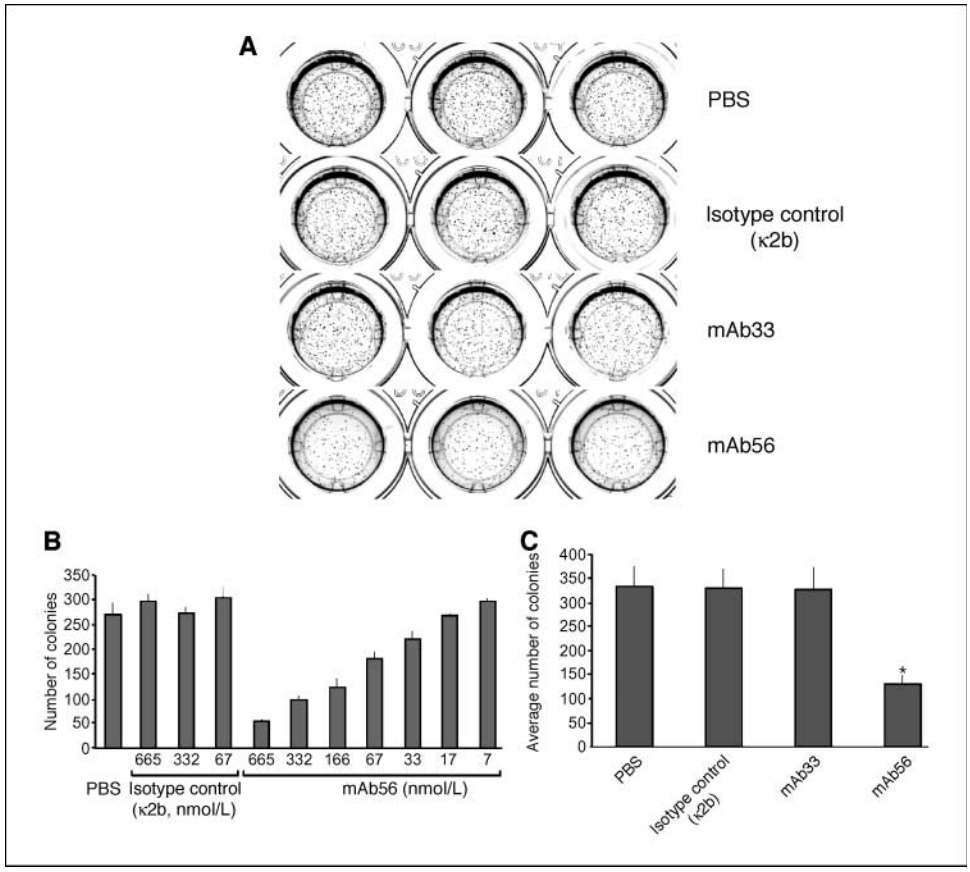

Figure 4. Anti-Eag1 monoclonal antibody mAb56 inhibits anchorage-independent cancer cell growth *in vitro. A,* colony formation was impaired by incubation with mAb56, but not by a control isotype antibody or mAb33 (against hEag1 COOH terminus). SKOV3 cells were preincubated with 133 nmol/L of mAb56, mAb33, antibody 4H1A7 (control mouse IgG), or PBS. *B,* the effect of mAb56 on the number of colonies shows dose-dependence. Average number of colonies in the presence of the listed concentrations (in nmol/L) of mAb3 (SKOV3 ovary carcinoma). *C,* average number of colonies in three independent experiments similar to the one in (*A*).

the same region, and whose epitope is located only 23 residues upstream of that of mAb56 (Fig. 1*A*), failed to reduce the hEag1 current under the same conditions (Fig. 2). Sequential application of the antibodies revealed that mAb56 effectively reduced the current amplitude in cells that had shown no response to mAb62 (Fig. 2*B*), although mAb62 was able to bind to the channels in intact cells, as shown in immunofluorescence experiments (Fig. 2*B, inset*). These results strongly indicate that antibody recognition of the E3 region was necessary but not sufficient to achieve channel inhibition (15). Thus, some additional features were required to obtain functional antibodies. The slow time course of the block could follow the combination of a limited diffusion rate due to the relatively large molecular weight of the antibody, and the need for depolarization to achieve the block because pulses were applied at a frequency of 3 Hz.

Current inhibition by mAb56 showed dose-dependence. Because each antibody concentration required long incubation periods to reach steady state (at least 10 min), and because of the large amounts of antibody required for these experiments, we only estimated the concentration for half-maximal inhibition. A free fit of the average inhibition using the Hill equation gave an IC_{50} value of mAb56 in HEK293 cells of 73 $\pm$ 47 nmol/L (Fig. 2*C*).

Table 1. Overall level of inhibition mediated by mAb56 at the indicated concentration in different human tumor cell lines of various origins

Origin	Cell line	Inhibition of colony formation (%)	Concentration (nmol/L)
Breast carcinoma	MDA-MB-435s	60	66
	NCI-ADR	25	166
Melanoma	HT144	35	133
	C8161	25	133
	SKMel2	35	133
Ovarian carcinoma	SKOV3	40	133
	OVCAR-3	25	133
	SKOV-6	35	266
	OVCAR-8	25	133
Cervical carcinoma	HeLa	40	133
Pancreas carcinoma	BxPC3	20–25	133
Colon carcinoma	HT29	30	66
Fibrosarcoma	HT1080	30–40	133

To show that the effects of mAb56 depend on specific binding to the channel through the complementarity-determining regions, we measured the current amplitude in the presence of mAb56 that had been preincubated with a molar excess of a peptide with the sequence of the corresponding epitope (Fig. 2*D*). This treatment abolished the effects of mAb56 on hEag1 currents, indicating that the inhibition of the current was mediated by binding through the complementarity-determining regions and was therefore specific. Preincubation with a peptide with the mAb62 epitope sequence did not have any effect (Fig. 2*D*).

mAb56 blocks the native hEag1 current in neuroblastoma cells. To determine if mAb56 also blocks native currents and not only heterologously expressed channels, we selected the human neuroblastoma cell line SH-SY5Y. Eag1 and Eag2 show a remarkable dependence of the activation time constant on the prepulse potential (Cole-Moore shift). The magnitude of this shift is so unique that it can be taken as unequivocal identification of the current carried by Eag1 and Eag2. The potassium currents recorded from SH-SY5Y cells clearly show this property (32) and are reduced by antisense oligonucleotides (7). These cells abundantly express hEag1 mRNA, but no RNA encoding hEag2 is detectable. Therefore, native homomeric hEag1 channels are probably responsible for the observed currents. These endogenous hEag1 currents (Fig. 3*A*) were also inhibited by ~45% after 5 min of mAb56 perfusion (300 nmol/L), indicating that not only heterologously expressed, but also native hEag1 can be inhibited by mAb56.

mAb56 does not affect currents through HERG channels. Because HERG blockade is a major concern for all potential pharmacologic compounds and, even more acutely, for ion channel blockers (19), we tested whether mAb56 affects the amplitude of currents flowing through HERG channels.

Perfusion of mAb56 (~300 nmol/L) did not show any reduction on HERG currents expressed in HEK293 cells (Fig. 3*B*), showing that mAb56 selectively blocks ion channel flow mediated by hEag1 but not by HERG. Note that the small reduction in current seen in Fig. 3*B* is probably mere rundown because it occurs at the same rate in the presence or absence of antibody.

Therefore, mAb56 is the only known molecule able to inhibit hEag1 whereas leaving HERG unaffected. This finding reinforces the concept that monoclonal antibodies may represent an alternative to traditional ion channel blockers when blockade of a related molecule represents a concern.

mAb56 inhibits the growth of tumor cells. To analyze the biological consequences of hEag1 blockade by mAb56, we tested the effects of mAb56 on tumor cell growth under nonadherent culture conditions. The ability of tumor cells to form colonies in soft agar is an indication for the transformation of the cells because anchorage-independent cell growth is characteristic of tumor cells. As shown in Fig. 4*A*, mAb56 significantly impaired the ability of SKOV3 ovarian carcinoma cells to form colonies in soft agar in a concentration-dependent manner (Fig. 4*B*). The addition of PBS, a control isotype antibody (κ2b) or another monoclonal antibody against the COOH-terminal region of hEag1 (mAb33) did not influence colony formation (Fig. 4*C*), suggesting that mAb56-mediated hEag1 blockade exerts antiproliferative activity *in vitro*.

Similar experiments were done in several tumor cell lines from different types of cancer (all of which express abundant hEag1). mAb56 extensively reduced growth in all tested lines (Table 1). Together with the exquisite specificity against hEag1 shown by mAb56, these results reinforce the concept that hEag1 exerts a role in the proliferation of tumor cells.

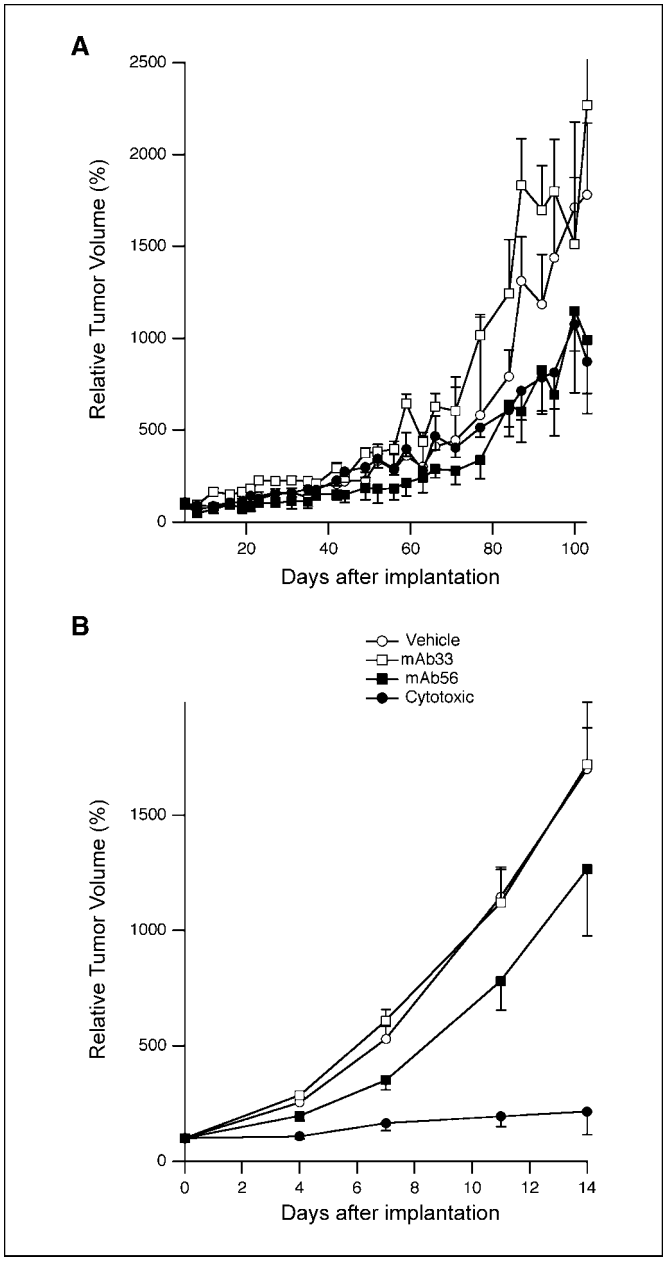

Figure 5. Anti-hEag1 monoclonal antibody mAb56 reduces tumor growth *in vivo*. *A,* MDA-MB-435s breast cancer xenograft model. After randomization, two groups of tumor-bearing SCID mice (10 mice/group) received mAb56 or mAb33 at a loading dose of 50 mg/kg and were followed by weekly doses of 25 mg/kg (i.p.). The chemotherapeutic control, cyclophosphamide (*cytotoxic*), was administered daily at a dose of 40 mg/kg (p.o.). The fourth group received vehicle (PBS). *B,* PAXF1657 primary pancreas cancer xenograft model. Two groups of tumor-bearing nude mice (10 mice/group) received mAb56 or mAb33 at a loading dose of 50 mg/kg and follow-up dosing of 25 mg/kg on days 4, 7, and 11. Gemcitabine (*cytotoxic*) was administered i.v. at 200 mg/kg on days 0 and 7. The fourth group received vehicle (PBS) on days 4, 7, and 11 (i.p.).

Efficacy of mAb56 on some tumor xenograft models. To explore the potential antitumor efficacy of anti-Eag1 antibodies *in vivo*, we administered mAb56 to SCID mice carrying s.c. tumors induced by xenografts of MDA-MB-435S human breast cancer cells. The antitumor activity of mAb56 was compared with an established chemotherapeutic control, cyclophosphamide. Two groups of animals received mAb56 or vehicle at a loading dose of 50 mg/kg followed by weekly dosing of 25 mg/kg (i.p. injections). In this study,

anti-Eag1 antibody treatment was as efficacious as standard chemotherapy in reducing tumor growth (Fig. 5*A*). It should be noted that mAb56, which is cross-reactive with mouse and rat Eag1 (data not shown), did not cause any obvious side effects like weight loss or neurologic abnormalities in treated animals. In contrast with MDA-MB-435S xenografts, anti-Eag1 antibodies were not efficacious in SKOV3 ovarian cancer and BxPC3 pancreatic cancer xenograft studies (data not shown). It is interesting to note that the loading dose of 50 mg/kg, which represents 1 mg of antibody for a 20 g animal, will probably render plasma concentrations <20 mg/mL, which corresponds to the 300 nmol/L used in electrophysiology; further dosage exploration will be required in these models. Furthermore, at least in case of BxPC3 tumor cells, the lack of an *in vivo* antitumor effect correlated with very low expression levels of hEag1 in the xenograft tissue, which did not match the expression levels detected *in vitro* (data not shown).

We further investigated the antitumor activity of mAb56 in a primary model of human cancer. PAXF1657 tumors were derived directly from a human pancreatic cancer patient and were maintained continuously as s.c. xenografts in nude mice. Thus, PAXF1657 xenografts are assumed to closely resemble the malignant pancreatic cancer phenotype observed in the clinic. PAXF1657-bearing mice were treated with mAb56 and mAb33 (as a control) at a loading dose of 50 mg/kg followed by doses of 25 mg/kg on days 4, 7, and 11 of the study (i.p. injections). In this case, gemcitabine was included as a positive control. In this experiment, mAb56 inhibited tumor progression consistently in the range of 30% to 40% throughout the study duration (Fig. 5*B*). In contrast, treatment of animals with the functionally inactive anti-Eag1 antibody, mAb33, which is directed against the COOH-terminal region of the channel, had no influence on tumor growth *in vivo* (Fig. 5*B*). These results were confirmed in an additional independent PAXF1657 animal study (data not shown). These results further substantiate our finding that mAb56-mediated hEag1 ion channel current blockade exerts antitumor activity *in vivo*.

In conclusion, we have designed a rational strategy to generate a monoclonal antibody that functionally recognizes hEag1 ion channel protein and potently reduces hEag1 ion channel current. This strategy, which should be generally applicable, has produced the first monoclonal antibody able to inhibit an ion channel current in intact cells. The antibody is highly selective and does not bind to hEag2. Importantly, mAb56 does not affect HERG current. Therefore, mAb56 represents the first specific inhibitor of the hEag1 channel and will serve as a unique tool to elucidate the role of hEag1 channels in physiologic and pathologic processes. In addition, by blocking hEag1 ion channel activity, mAb56 effectively impairs tumor cell growth *in vitro* and *in vivo*, confirming the link between hEag1 expression and the proliferation properties of cancerous cells and tumor growth.

Acknowledgments

Received 1/10/2007; revised 4/20/2007; accepted 5/22/2007.

Grant support: Funded in part by the German Federal Ministry of Education and Research, Bio Chance program.

The costs of publication of this article were defrayed in part by the payment of page charges. This article must therefore be hereby marked *advertisement* in accordance with 18 U.S.C. Section 1734 solely to indicate this fact.

We thank Victor Diaz, Michaela Hellwig, Kerstin Dehne, and Yvonne Riffner for technical assistance.

References

1. Ashcroft FM. From molecule to malady. Nature 2006;440:440–7.
2. Pardo LA. Voltage-gated potassium channels in cell proliferation. Physiology 2004;19:285–92.
3. Pardo LA, Contreras-Jurado C, Zientkowska M, Alves F, Stühmer W. Role of voltage-gated potassium channels in cancer. J Membr Biol 2005;205:115–24.
4. Gutman GA, Chandy KG, Grissmer S, et al. International Union of Pharmacology. LIII. Nomenclature and molecular relationships of voltage-gated potassium channels. Pharmacol Rev 2005;57:473–508.
5. Pardo LA, Brüggemann A, Camacho J, Stühmer W. Cell cycle-related changes in the conducting properties of r-eag K^+ channels. J Cell Biol 1998;143:767–75.
6. Brüggemann A, Stühmer W, Pardo LA. Mitosis-promoting factor-mediated suppression of a cloned delayed rectifier potassium channel expressed in Xenopus oocytes. Proc Natl Acad Sci U S A 1997;94:537–42.
7. Pardo LA, del Camino D, Sánchez A, et al. Oncogenic potential of EAG K^+ channels. EMBO J 1999;18:5540–7.
8. Weber C, Mello de Queiroz F, Downie B, Sukow A, Stühmer W, Pardo LA. Silencing the activity and proliferative properties of the human Eag1 potassium channel by RNAi. J Biol Chem 2006;281:13033–7.
9. Gavrilova-Ruch O, Schönherr K, Gessner G, et al. Effects of imipramine on ion channels and proliferation of IGR1 melanoma cells. J Membr Biol 2002;188:137–49.
10. Ouadid-Ahidouch H, Le Bourhis X, Roudbaraki M, Toillon RA, Delcourt P, Prevarskaya N. Changes in the K^+ current-density of MCF-7 cells during progression through the cell cycle: possible involvement of a h-ether.a-gogo K^+ channel. Receptors Channels 2001;7:345–56.
11. Farias LMB, Bermúdez Ocaña D, Díaz L, et al. Ether à go-go potassium channels as human cervical cancer markers. Cancer Res 2004;64:6996–7001.
12. Hemmerlein B, Weseloh RM, Mello de Queiroz F, et al. Overexpression of Eag1 potassium channels in clinical tumour specimens. Mol Cancer 2006;5:41.
13. Mello de Queiroz F, Suarez-Kurtz G, Stühmer W, Pardo LA. Ether à go-go potassium channel expression in soft tissue sarcoma patients. Mol Cancer 2006;5:42.
14. Occhiodoro T, Bernheim L, Liu JH, et al. Cloning of a human ether-a-go-go potassium channel expressed in myoblasts at the onset of fusion. FEBS Lett 1998;434:177–82.
15. Xu SZ, Zeng F, Lei M, et al. Generation of functional ion-channel tools by E3 targeting. Nat Biotechnol 2005;23:1289–93.
16. Ju M, Wray D. Molecular identification and characterisation of the human eag2 potassium channel. FEBS Lett 2002;524:204–10.
17. Schönherr R, Gessner G, Lober K, Heinemann SH. Functional distinction of human EAG1 and EAG2 potassium channels. FEBS Lett 2002;514:204–8.
18. Warmke JW, Ganetzki B. A family of potassium channel genes related to eag in Drosophila and mammals. Proc Natl Acad Sci U S A 1994;91:3438–42.
19. Sanguinetti MC, Tristani-Firouzi M. hERG potassium channels and cardiac arrhythmia. Nature 2006;440:463–9.
20. Zhou Z, Vorperian VR, Gong Q, Zhang S, January CT. Block of HERG potassium channels by the antihistamine astemizole and its metabolites desmethylastemizole and norastemizole. J Cardiovasc Electrophys 1999;10:836–43.
21. García-Ferreiro RE, Kerschensteiner D, Major F, Monje F, Stühmer W, Pardo LA. Mechanism of block of hEag1 K^+ channels by imipramine and astemizole. J Gen Physiol 2004;124:301–17.
22. Zhou BY, Ma W, Huang XY. Specific antibodies to the external vestibule of voltage-gated potassium channels block current. J Gen Physiol 1998;111:555–63.
23. Kim SJ, Park Y, Hong HJ. Antibody engineering for the development of therapeutic antibodies. Mol Cells 2005;20:17–29.
24. Brekke OH, Loset GA. New technologies in therapeutic antibody development. Curr Opin Pharmacol 2003;3:544–50.
25. Ludwig J, Owen D, Pongs O. Carboxy-terminal domain mediates assembly of the voltage-gated rat ether-a-go-go potassium channel. EMBO J 1997;16:6337–45.
26. Jenke M, Sánchez A, Monje F, Stühmer W, Weseloh RM, Pardo LA. C-terminal domains implicated in the functional surface expression of potassium channels. EMBO J 2003;22:395–403.
27. Taylor KM, Lin T, Porta C, et al. Influence of three-dimensional structure on the immunogenicity of a peptide expressed on the surface of a plant virus. J Mol Recognit 2000;13:71–82.
28. Karlsson R, Michaelsson A, Mattsson L. Kinetic analysis of monoclonal antibody-antigen interactions with a new biosensor based analytical system. J Immunol Methods 1991;145:229–40.
29. Stühmer W. Electrophysiological recordings from Xenopus oocytes. Methods Enzymol 1992;207:319–39.
30. Hamill OP, Marty A, Neher E, Sakmann B, Sigworth FJ. Improved patch-clamp techniques for high-resolution current recording from cells and cell-free membrane patches. Pflueg Arch Eur J Physiol 1981;391:85–100.
31. Napp J, Monje F, Stühmer W, Pardo LA. Glycosylation of Eag1 (Kv10.1) potassium channels: intracellular trafficking and functional consequences. J Biol Chem 2005;280:29506–12.
32. Meyer R, Heinemann SH. Characterization of an eag-like potassium channel in human neuroblastoma cells. J Physiol 1998;508:49–56.